JACS
JOURNAL OF THE AMERICAN CHEMICAL SOCIETY
Article
pubs.acs.org/JACS

# Protein Isotope Effects in Dihydrofolate Reductase From *Geobacillus stearothermophilus* Show Entropic–Enthalpic Compensatory Effects on the Rate Constant

Louis Y. P. Luk,[†,#] J. Javier Ruiz-Pernía,[§,#] William M. Dawson,[†] E. Joel Loveridge,[†] Iñaki Tuñón,[*,‡] Vicent Moliner,[*,§] and Rudolf K. Allemann[*,†,∥]

[†]School of Chemistry and [∥]Cardiff Catalysis Institute, School of Chemistry, Cardiff University, Park Place, Cardiff, CF10 3AT, United Kingdom

[‡]Departament de Química Física, Universitat de València, 46100 Burjassot, Spain

[§]Departament de Química Física i Analítica, Universitat Jaume I, 12071 Castelló, Spain

Supporting Information

**ABSTRACT:** Catalysis by dihydrofolate reductase from the moderately thermophilic bacterium *Geobacillus stearothermophilus* (BsDHFR) was investigated by isotope substitution of the enzyme. The enzyme kinetic isotope effect for hydride transfer was close to unity at physiological temperatures but increased with decreasing temperatures to a value of 1.65 at 5 °C. This behavior is opposite to that observed for DHFR from *Escherichia coli* (EcDHFR), where the enzyme kinetic isotope effect increased slightly with increasing temperature. These experimental results were reproduced in the framework of variational transition-state theory that includes a dynamical recrossing coefficient that varies with the mass of the protein. Our simulations indicate that BsDHFR has greater flexibility than EcDHFR on the ps–ns time scale, which affects the coupling of the environmental motions of the protein to the chemical coordinate and consequently to the recrossing trajectories on the reaction barrier. The intensity of the dynamic coupling in DHFRs is influenced by compensatory temperature-dependent factors, namely the enthalpic barrier needed to achieve an ideal transition-state configuration with minimal nonproductive trajectories and the protein disorder that disrupts the electrostatic preorganization required to stabilize the transition state. Together with our previous studies of other DHFRs, the results presented here provide a general explanation why protein dynamic effects vary between enzymes. Our theoretical treatment demonstrates that these effects can be satisfactorily reproduced by including a transmission coefficient in the rate constant calculation, whose dependence on temperature is affected by the protein flexibility.

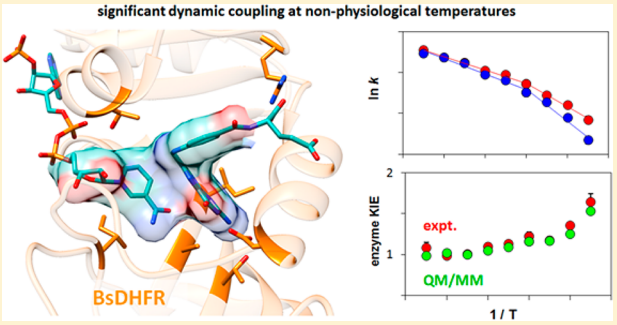


## INTRODUCTION

Kinetic investigation of isotopically substituted enzymes has led to major advances of our understanding of enzyme-catalyzed reactions.[1−9] When nonexchangeable hydrogen, carbon, and nitrogen atoms in an enzyme are replaced by heavier counterparts (e.g., $^{15}$N, $^{13}$C, $^{2}$H), mass-dependent protein motions from bond vibrations to protein loop or domain movements are slowed.[2,5,10] Consequently, the effect(s) of the protein environmental coordinate can be revealed by the reactivity difference between the 'heavy' (isotopically substituted) and 'light' (natural isotopic abundance) enzymes. Protein motions have been postulated to be crucial for enzyme catalysis by coupling to the substrate as a strategy to reduce the energy of barrier crossing.[11] It was hypothesized that enzymes operate by generating nonstatistical motions to promote chemical transformations.[12−16] These theoretical frameworks however have been challenged by others who suggested that most protein motions are already thermally dissipated during the chemical transformation step.[17−19] Numerous experimental and theoretical approaches have been used to explore the effect of protein dynamics on enzyme catalysis.[18,20−34] Among these, enzyme isotope substitution is one of the most sensitive in revealing the role of motions on time scales from femtoseconds to milliseconds.

Dihydrofolate reductase (DHFR) has become a paradigmatic model for the study of enzyme catalysis. DHFR catalyzes the transfer of the pro-*R* hydride from the C4 position of NADPH and a proton from water to the C6 and N5 positions of dihydrofolate ($H_2F$), respectively. While millisecond conformational changes involved in ligand binding and release are often essential for progression through the catalytic cycle,[32,35] the actual role of protein dynamics in the step of chemical transformation remains a subject of debate. Previously, the dynamic properties of DHFR from *Escherichia coli* (EcDHFR), the catalytically compromised mutant EcDHFR-N23PP/S148A

**Received:** October 6, 2014
**Published:** November 14, 2014

   dx.doi.org/10.1021/ja5102536 | J. Am. Chem. Soc. 2014, 136, 17317−17323

and DHFR from *Thermotoga maritima* (TmDHFR) have been investigated by enzyme isotope substitution.[6−9] For EcDHFR a small, temperature-dependent isotope effect on the step of the chemical transformation was observed,[6,7] but for EcDHFR-N23PP/S148A this effect was noticeably stronger.[8] In contrast, catalysis by TmDHFR is not sensitive to protein isotope substitution.[9] Quantum mechanical/molecular mechanical (QM/MM) calculations revealed that the observed dynamic coupling in EcDHFR originates from protein environmental motions on the fs−ps time scale, which exert an effect on the reaction trajectories.[7,8] These motions however do not promote catalysis by reducing the height or width of the barrier to hydride transfer by means of nonstatistical fluctuations. Indeed, as demonstrated in the investigation of EcDHFR-N23PP/S148A, protein dynamic effects due to motions that cannot be considered in equilibrium with the reaction coordinate have a larger impact on catalysis in this mutant than in the wild type, as reflected in the enhanced probability of nonproductive reaction trajectories.[8] These results together suggested that dynamic effects should be minimized in DHFR because its active site has been better preorganized for catalysis. Nevertheless, protein isotope effects clearly vary among these enzymes and additional analysis is needed to fully understand their role in enzyme catalyzed hydrogen transfer reactions.

During catalytic turnover, EcDHFR alternates between the closed and occluded conformations through the coordinated movements of the M20, FG, and GH loops.[35] The hyperthermphilic TmDHFR however is locked in the open conformation due to its dimeric structure; the M20 and FG loops are buried in the interface between the subunits.[36] DHFR from *Geobacillus stearothermophilus* (BsDHFR) is a moderately thermophilic monomeric enzyme with an optimal functional temperature of ∼60 °C (Figure 1).[37,38] Thermal adaptation in

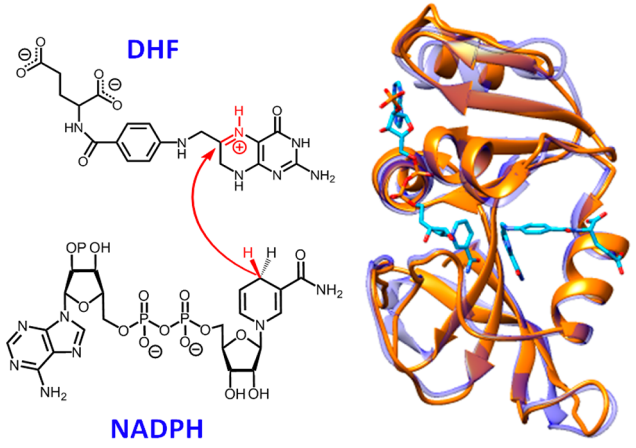


**Figure 1.** Conversion of dihydrofolate to tetrahydrofolate through transfer of the pro-*R* hydride of NADPH. Overlay of the X-ray structures of BsDHFR (gold) (PDB 1ZDR)[37] and EcDHFR (blue) (PDB 1RX2).[35]

BsDHFR is achieved by the removal of 'thermolabile' residues and the extension of secondary structural elements.[37,38] In contrast to many other thermophilic and mesophilic enzyme pairs, BsDHFR has been suggested to be more flexible than the mesophilic EcDHFR on the ns time scale.[22,39] While the catalytic properties of BsDHFR are similar to those of EcDHFR,[37,38] there is no experimental evidence indicating that BsDHFR can adopt an occluded conformation during catalysis.[37] Here we compare the kinetic properties of 'heavy' and 'light' BsDHFR; at low temperature an enzyme kinetic isotope effect (KIE) of approximately 60% was observed due to coupling of environmental motions to the chemical step, while at elevated temperatures the kinetic properties for both 'light' and 'heavy' BsDHFR were largely identical.

## RESULTS AND DISCUSSION

Perdeuterated, $^{13}C$, $^{15}N$ doubly labeled and $^{13}C$, $^{15}N$, $^{2}H$ triply labeled BsDHFRs were produced in M9 minimal media containing the appropriate isotopically labeled ingredients (see Supporting Information (SI)). Both perdeuterated and $^{13}C$, $^{15}N$ labeled BsDHFRs showed a molecular weight (MW) increase of 5.5%, whereas the MW increase of the $^{13}C$, $^{15}N$, $^{2}H$ triply labeled ('heavy') BsDHFR is 11.1% (in this article, 'heavy' BsDHFR only refers to the triply labeled enzyme). In all cases, this shows that at least 99.5% of the relevant nonexchangeable atoms in BsDHFR were replaced by their heavy counterparts (Figure S1).

At neutral pH, physical steps in the catalytic cycle of BsDHFR are mostly rate-limiting.[37,38] The steady-state turnover rate constants for 'light' BsDHFR, $k_{cat}^{LE}$, are considerably higher than those measured for the triply labeled, 'heavy' BsDHFR, $k_{cat}^{HE}$ (Figure S2, Tables S1 and S2) and a large and relatively constant enzyme $KIE_{cat}$ ($k_{cat}^{LE}/k_{cat}^{HE}$) of approximately 2.6 was obtained across the examined temperature range (7−45 °C). For the perdeuterated and $^{13}C$, $^{15}N$ doubly labeled BsDHFRs, the corresponding average values for the enzyme $KIE_{cat}$ are noticeably lower (∼1.6 and 1.9, respectively) than that observed for 'heavy' BsDHFR. Also, the Michaelis constants, $K_M$, for both NADPH and dihydrofolate were not affected markedly by isotope substitution at all tested temperatures (10, 20, and 35 °C, Table S3). Hence, the observed enzyme isotope effect on $k_{cat}$ is unlikely to be a consequence of altered ligand binding.

The steady-state enzyme KIEs presented here were considerably larger than those measured for other DHFR homologues.[7−9] In EcDHFR, the measured enzyme KIE on the overall turnover ($KIE_{cat}$) increased from unity at 10 °C to 1.15 at 40 °C and was attributed to the rate-limiting conformational change necessary for the release of dihydrofolate.[7,8,35,40] The temperature-independent enzyme KIEs on $k_{cat}$ at pH 7.0 observed for the catalytically compromised mutant EcDHFR-N23PP/S148A (∼1 for all temperatures measured)[8] and TmDHFR (∼1.37 for temperatures above 20 °C)[9] agree well with the fact that large conformational changes are absent in these enzymes.[32,36] Accordingly, the temperature-independent enzyme $KIE_{cat}$ in BsDHFR is not likely to be caused by a rate-limiting conformational switch. Instead, the relatively large enzyme isotope effect may report on the previously observed inherent flexibility of this enzyme.[22,39]

Hydride transfer from reduced NADPH to dihydrofolate at physiological pH was monitored in pre-steady-state stopped-flow experiments. While isotopic substitution of BsDHFR did not affect the apparent $pK_a$ value of the reaction (Figure S3, Table S4), the enzyme $KIE_H$ ($k_H^{LE}/k_H^{HE}$) at pH 7 showed an inverse dependence on temperature (Figure 2A,C, Tables S1 and S2). At temperatures above 20 °C, the enzyme $KIE_H$ is only weakly dependent on temperature, with a value of <1.10, but it rises sharply with decreasing temperature such that at 5 °C the hydride transfer rate constant for the 'heavy' BsDHFR is only 60% of that of the 'light' counterpart.


dx.doi.org/10.1021/ja5102536 | J. Am. Chem. Soc. 2014, 136, 17317−17323

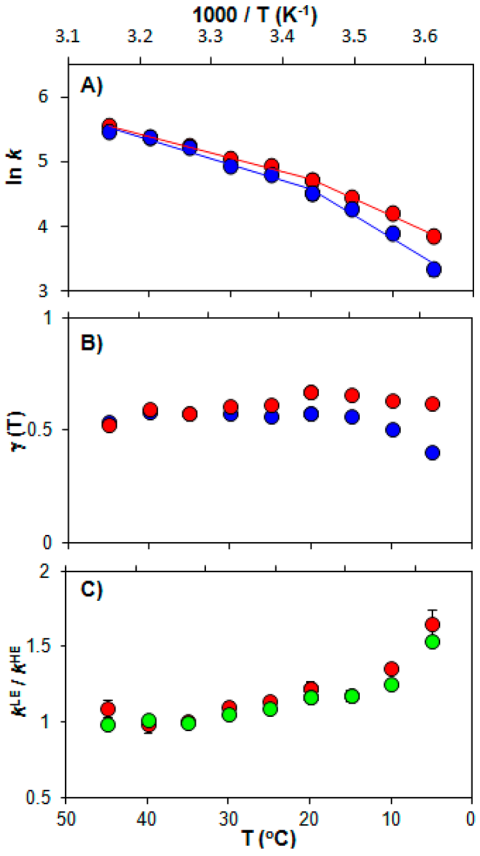


**Figure 2.** Experimental and computational data for the hydride transfer reaction catalyzed by BsDHFR. (A) Temperature dependence of the pre-steady-state rate constants for hydride transfer catalyzed by 'light' (red) and 'heavy' (blue) BsDHFR at pH 7.0, (B) their corresponding recrossing coefficients ($\gamma(T)$) and (C) enzyme KIE ($k^{LE}/k^{HE}$) from experiments (red) and calculations (green).

The enzyme isotope effects were also evaluated for the perdeuterated and $^{13}C$, $^{15}N$ doubly labeled BsDHFRs, the MWs of which were increased by only half that of the triply labeled 'heavy' enzyme. Between 15 and 45 °C the calculated isotope effects are statistically the same as those measured for 'heavy' BsDHFR (Figure S2, Table S1 and S2). These results are in agreement with a view of enzyme chemistry in which dynamic coupling under physiological conditions is minimized,[7−9] because the values of the enzyme $KIE_H$ obtained for the perdeuterated and doubly ($^{13}C$, $^{15}N$) labeled BsDHFRs are already close to that of the fully labeled 'heavy' enzyme. In contrast, at 5 °C the enzyme $KIE_H$ values for singly (1.42 ± 0.05) and doubly labeled (1.24 ± 0.04) BsDHFRs are lower than that of the fully labeled enzyme (1.65 ± 0.09). The observed enzyme $KIE_H$ are mainly caused by a change in protein dynamics, rather than other mass-induced effects such as a drop in the van der Waals radii on deuterium labeling. Furthermore, the CD spectra and the thermal melting temperature curves for 'light' and 'heavy' BsDHFR were essentially identical under various buffer concentrations (10, 20, 50 mM $KP_i$ at pH 7.0, Figure S4). In a recent study of EcDHFR, it was proposed that the ground-state conformational ensemble of the enzyme was altered by heavy isotope labeling, because there were measurable changes in ligand binding affinities and thermal melting temperatures.[6] Our results show that while heavy isotope labeling might lead to some changes to the ground-state conformational ensemble of BsDHFR, altered dynamics in the triply labeled, 'heavy' BsDHFR make a significant contribution to the observed enzyme kinetic isotope effects $KIE_H$.

To gain further understanding of the nature of the dynamic coupling and the unique temperature dependence of the enzyme KIEs found in BsDHFR, QM/MM ensemble averaged variational transition state theory (EA-VTST) calculations were carried out at different temperatures (Figure 3). The theoretical

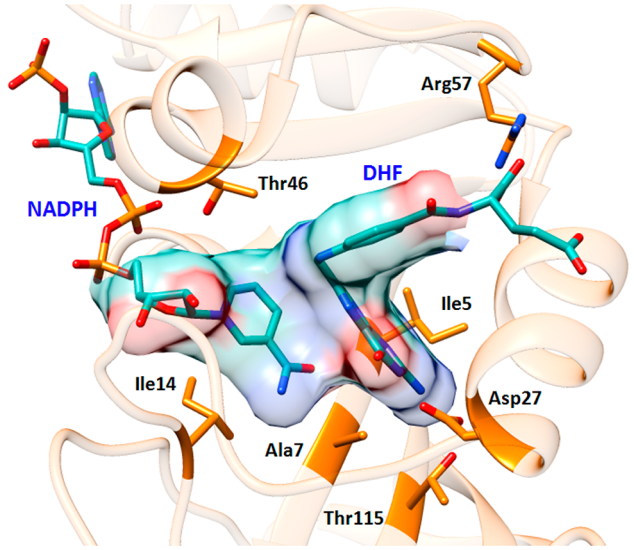


**Figure 3.** Representation of the active site of BsDHFR. Substrate DHF, cofactor NADPH, and key amino acid residues are shown as sticks. The portion of the reactants treated quantum mechanically in the QM/MM simulations (SI text and Figure S5) is shown with an overlaid surface representation. The figure was created from PDB file 1ZDR.[37]

calculation of the rate constants of the chemical step was based on TST modified to account for tunneling contributions and dynamic effects:[41−43]

$$k_{\text{theor.}}(T) = \Gamma(T)\frac{k_B T}{h} e^{-\left(\frac{\Delta G_{act}^{QC}(T)}{RT}\right)} = \frac{k_B T}{h} e^{-\left(\frac{\Delta G_{eff}(T)}{RT}\right)} \quad (1)$$

where $R$ is the ideal gas constant, $T$ is the temperature, $k_B$ is the Boltzmann constant, $h$ is Planck's constant, $\Delta G_{act}^{QC}$ is the quasiclassical activation free energy,[44] $\Delta G_{eff}$ is the effective activation free energy (for details see SI) and $\Gamma(T)$ is the temperature-dependent transmission coefficient. $\Gamma(T)$ contains dynamic and tunneling corrections to the classical rate constant and is therefore equal to one in the limit of classical TST. $\Gamma(T)$ can be expressed as

$$\Gamma(T) = \gamma(T)\cdot\kappa(T) \quad (2)$$

where $\gamma(T)$ is the recrossing transmission coefficient that corrects the rate constant for the trajectories that recross the dividing surface from the product valley back to the reactant valley, and $\kappa(T)$ is the tunneling coefficient that accounts for reactive trajectories that do not reach the classical threshold energy. All parameters in eqs 1 and 2 can be obtained from QM/MM simulations (for details see SI), as has been described previously for the analyses of EcDHFR and its catalytically compromised variant EcDHFR-N23PP/S148A.[7,8]

Classical potentials of mean force (PMF) were computed separately at 278, 298, and 318 K. The PMFs traced as a function of the selected reaction coordinate (the antisymmetric


dx.doi.org/10.1021/ja5102536 | J. Am. Chem. Soc. 2014, 136, 17317−17323

**Table 1. Temperature Dependence of Transmission Coefficient Components Due to Recrossing ($\gamma$) and Tunneling ($\kappa$), Quasi-Classical (QC) Free Energy of Activation ($\Delta G_{act}^{QC}$), Effective Phenomenological Free Energies of Activation ($\Delta G_{eff}$), and Hydride Transfer Rate Constants in 'Light' And 'Heavy' BsDHFR Determined by QM/MM Calculations ($k_{theor.}$) and Stopped-Flow Measurements ($k_H$)**

| $T$ (K) | BsDHFR | $\gamma$ | $\kappa$ | $\Delta G_{act}^{QC}$(kcal mol$^{-1}$) | $\Delta G_{eff}$ (kcal mol$^{-1}$) | $k_{theor.}$ (s$^{-1}$) | $(k^{LE}/k^{HE})_{theor.}$ | $k_H$ (s$^{-1}$) | $(k_H^{LE}/k_H^{HE})_{exp.}$ |
|---|---|---|---|---|---|---|---|---|---|
| 278 | light | 0.62 ± 0.02 | 4.2 ± 0.5 | 13.15 ± 0.58 | 12.62 ± 0.58 | 690 | 1.53 ± 0.09 | 46.7 ± 3.2 | 1.65 ± 0.09 |
| | heavy | 0.40 ± 0.02 | | | 12.86 ± 0.58 | 450 | | 28.3 ± 2.5 | |
| 298 | light | 0.61 ± 0.02 | 3.5 ± 0.3 | 13.74 ± 0.51 | 13.29 ± 0.51 | 1120 | 1.10 ± 0.04 | 139.5 ± 2.4 | 1.14 ± 0.02 |
| | heavy | 0.56 ± 0.01 | | | 13.34 ± 0.51 | 1020 | | 122.2 ± 4.0 | |
| 318 | light | 0.53 ± 0.02 | 2.9 ± 0.5 | 14.11 ± 0.57 | 13.85 ± 0.58 | 2020 | 0.98 ± 0.04 | 256.3 ± 12 | 1.09 ± 0.06 |
| | heavy | 0.53 ± 0.01 | | | 13.84 ± 0.58 | 2050 | | 235.3 ± 7.2 | |

**Table 2. Kinetic Parameters for the Hydride Transfer Reactions Catalyzed by the 'Light' And 'Heavy' BsDHFRs at 25 °C and Comparison to Other DHFRs**

| | $\Delta S^{\ddagger}$ (cal·mol$^{-1}$·K$^{-1}$) | | $\Delta H^{\ddagger}$ (kcal·mol$^{-1}$·K$^{-1}$) | | $\Delta G^{\ddagger}$ (kcal·mol$^{-1}$·K$^{-1}$) | $E_A$ (kcal·mol$^{-1}$·K$^{-1}$) |
|---|---|---|---|---|---|---|
| enzyme | exp. | QM/MM | exp. | QM/MM | exp. | exp. |
| light BsDHFR (5–45 °C) | −27 ± 2 | −31 ± 12 | 6.5 ± 0.3 | 4.1 ± 0.5 | 14.6 ± 1.6 | 7.2 ± 0.3 |
| heavy BsDHFR (5–45 °C) | −21 ± 2 | −25 ± 12 | 8.4 ± 0.6 | 6.1 ± 0.5 | 14.7 ± 1.8 | 9.0 ± 0.6 |
| light EcDHFR (5–40 °C)[a] | −26 ± 1 | NA | 6.7 ± 0.3 | NA | 14.4 ± 1.5 | 7.3 ± 0.2 |
| heavy EcDHFR (5–40 °C)[a] | −30 ± 2 | NA | 5.4 ± 0.6 | NA | 14.4 ± 2.5 | 6.0 ± 0.3 |
| light EcDHFR-N23PP/S148A (5–40 °C)[b] | −32 ± 2 | NA | 5.9 ± 0.3 | NA | 15.3 ± 1.8 | 6.5 ± 0.1 |
| heavy EcDHFR- N23PP/S148A (5–40 °C)[b] | −33 ± 3 | NA | 5.5 ± 0.3 | NA | 15.5 ± 2.8 | 6.1 ± 0.1 |
| light TmDHFR (5–40 °C)[c] | −23 ± 1 | NA | 11.7 ± 0.1 | NA | 18.4 ± 1.3 | 12.3 ± 0.3 |
| heavy TmDHFR (5–40 °C)[c] | −23 ± 1 | NA | 11.7 ± 0.1 | NA | 18.4 ± 1.9 | 12.3 ± 0.6 |

[a]Data obtained from ref 7. [b]Data obtained from ref 8. [c]Data obtained from ref 9.

combination of the distances of the hydride to the donor and to the acceptor atoms) are shown in Figure S6. The averaged value of the classical PMFs at each temperature was used to calculate the quasi-classical activation free energies (Table 1) after addition of quantum corrections to vibrational motions (see SI). The transition state (TS) and reactant averaged geometries were obtained from the windows corresponding to the maxima and minima of these PMFs. The majority of the geometric parameters are statistically the same at all examined temperatures (Table S5), and they are also similar to those computed previously for EcDHFR at 300 K.[7] However, some subtle temperature-dependent variations in the reactant state of BsDHFR were found in the distances between the cofactor and certain residues of the active site. While $d(HN2_{cofac} - O_{ALA7})$ increases, $d(HN1_{cofac} - O_{ILE14})$ decreases with rising temperature (see Figure S5 for the definition of the atoms). Furthermore, there is a small systematic displacement of the TS position along the reaction coordinate ($d(C4_{cofac} - H_t) - d(C6_{subs} - H_t)$) as temperature increases. Such a difference is consistent with the systematic increase in the height of the PMF maximum (Figure S6 and Table S6) and in the quasi-classical activation free energy (Table 1). Nevertheless, these structural differences are generally too small to cause the dramatic temperature-dependent change found experimentally for the enzyme KIEs.

Theoretical estimations of the rate constants ($k_{theor.}$) and the transmission coefficients were computed according to eq 1 and are collected in Table 1. The values for $k_{theor.}$ are generally larger than those measured experimentally. This is most likely due to an underestimation of the free energy barrier during the PMF computations. However, in terms of the activation free energy, the difference between the experimental values for $\Delta G^{\ddagger}$ (Table 2) and the theoretical effective activation free energies $\Delta G_{eff}$ (Table 1) is only approximately 1 kcal·mol$^{-1}$, which is well within the theoretical statistical deviations of the free energy calculations and the experimental errors. Hence, our computations provide a reasonably accurate illustration of the TS of the BsDHFR catalyzed reaction.

The tunneling contributions ($\kappa$) are identical in the light and heavy enzymes at all temperatures (Table 1). This observation is in agreement with our recent computational and experimental studies of other DHFR homologues, which indicated that tunneling or barrier modulation is not driven by compressive "promoting motions".[7−9] The difference in hydride transfer rate constants between the 'light' and 'heavy' enzymes arises solely from changes in the recrossing coefficients $\gamma$. To fully characterize the temperature dependence of the enzyme KIEs, nine pairs of recrossing transmission coefficients were computed from 278 to 318 K (Figure 2B, Tables S7 and S8). Although our calculations do not exclude other possible minor contributions, such as the enzyme isotope effect on changing the zero point energy of protein modes going from reactant to the TS, or a minimal structural change induced by a reduction in the vibrational averaged bond distances involving isotopically substituted atoms, our results demonstrate that the experimental enzyme KIE for $k_H$ can be reproduced from the calculated transmission coefficients (Table 1 and Figure 2C). These results are in excellent agreement with the experimental data, with the computational enzyme $KIE_H$ $(k^{LE}/k^{HE})_{theor.}$ also being relatively large at low temperatures and close to unity in the physiological temperature region. The recrossing transmission coefficient introduces a quantitatively minor correction to the calculated rate constant (a factor of ∼1.5), demonstrating the reliability of TST assumptions in the analysis of this enzymatic reaction. However, this dynamic correction is essential to explain small effects such as the enzyme KIEs (see SI and Figure S7). According to this analysis, it is not necessary to invoke other large nonstatistical motions of the protein to explain the change in the rate constant between the light and heavy versions of the enzyme.


dx.doi.org/10.1021/ja5102536 | J. Am. Chem. Soc. 2014, 136, 17317−17323

It should be noted that the reaction coordinate is defined exclusively in terms of the substrate and cofactor, which are unaffected by the isotope substitution of the enzyme. Consequently, the change in the recrossing transmission coefficient $\gamma$ reflects the subtle coupling of protein environmental motions to the reaction coordinate at TS. When the mass of the enzyme increases, protein motions are slower and less efficient in adapting to the progress of the system along the reaction coordinate. In other words, progression of the system along the reaction coordinate is slowed by increased friction in 'heavy' BsDHFR. This in turn leads to an increase in the number of recrossing events, a stronger deviation of $\gamma$ from unity, and consequently a drop in the rate constant for the 'heavy' enzyme catalyzed hydride transfer reaction.

As the magnitude of the enzyme $KIE_H$ for BsDHFR is noticeably larger than that for EcDHFR at low temperature,[7] the coupling of protein environmental motions to the reaction coordinate must be enhanced in the thermophilic enzyme. This could be the result of greater flexibility in BsDHFR. To test this proposal, the root mean square fluctuations (RMSF) of the $C^{\alpha}$ atoms in BsDHFR were calculated via 2 ns QM/MM MD simulations of the reactant state. The RMSF values are plotted in Figure 4 as a function of the residue number and compared

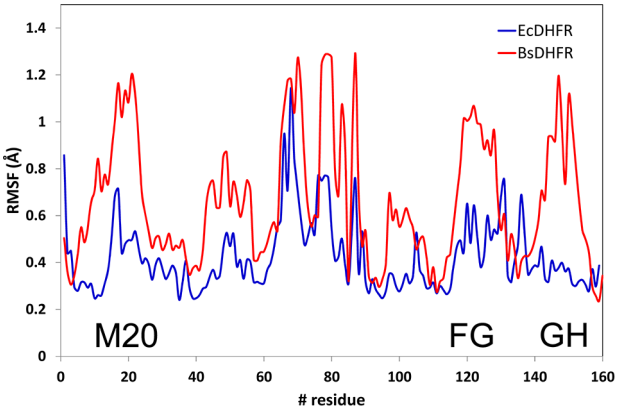


**Figure 4.** RMSF obtained for the C$\alpha$ atoms of BsDHFR (red) and EcDHFR (blue) from 2 ns QM/MM MD simulations of the reactants state at 298 K. The positions of the M20, FG and GH loops are indicated.

with those obtained for EcDHFR. The values for BsDHFR are systematically higher than those for EcDHFR, confirming that the thermophilic enzyme is more flexible on the ps−ns time scale, particularly in the M20, FG, and GH loops.

The temperature dependence of the enzyme $KIE_H$ can therefore be explained by a mass-induced effect on the recrossing coefficient (Figure 2B,C). While the magnitude of the recrossing coefficient in the 'light' enzyme is only mildly temperature-dependent, the corresponding parameter in 'heavy' BsDHFR decreases sharply at low temperatures. We hypothesize that the magnitude of the dynamic transmission coefficient is attributed to three temperature-dependent factors. The first factor refers to the energy associated with the reaction coordinate, which increases with temperature and elevates the recrossing coefficient close to unity. In contrast, the second factor, the thermal activation of other motions also increases with temperature but can lead to an increase in the number of recrossings and thus to a diminution of the transmission coefficient. Finally, one should also take into account the fact that the structure of the protein becomes progressively disordered when temperature increases. This entropic effect could perturb the process of electrostatic preorganization, raising the energy barrier for active site reorganization and causing the resulting transition from reactants to TS to contain additional protein environmental fluctuations. This leads to a reduced value of the recrossing transmission coefficient. In the case of BsDHFR, the slower protein motions caused by heavy isotope substitution are compensated for when increasing the temperature, which provides sufficient energy along the reaction coordinate for the enzyme to reach a transmission coefficient value close to that of the 'light' version. This unique ability of BsDHFR is probably accounted for by its inherent flexibility.

Evidence supporting this hypothesis can be found in the activation parameters (enthalpy and entropy) calculated based on the experimental hydride transfer rate constants and the temperature dependence of the computational $\Delta G_{eff}$ (Table 2). In our theoretical treatment (eq 1) these differences are due to changes in the transmission coefficient. The 'light' enzyme is energetically more capable of providing a configuration conducive to hydride transfer, as both the experimental and theoretical activation enthalpies ($\Delta H^{\ddagger}$) are ~2 kcal·mol$^{-1}$ lower than those for hydride transfer by the 'heavy' enzyme. Furthermore, the magnitude of the activation entropy ($\Delta S^{\ddagger}$) is also changed upon enzyme isotope substitution. Considering that the active site provides a complementary charge distribution for the TS, and such interactions require the surrounding residues to be ordered, a negative activation entropy is expected. However, the activation entropy for hydride transfer by the 'heavy' enzyme is significantly lower in magnitude than that for the 'light' version (Table 2). The differences in the activation parameters between the two versions of the enzyme can be analyzed in terms of the contributions due to the recrossing transmission coefficient. Based on the definition of the effective activation free energy (see eq 1), the dependency of the activation entropy on the recrossing coefficient can be expressed in the following manner:

$$\Delta S_{\gamma}^{\ddagger} = R\cdot\ln(\gamma) + \frac{RT}{\gamma}\cdot\frac{\partial\gamma}{\partial T} \qquad (3)$$

The first term $R\cdot\ln(\gamma)$ makes a negative contribution to the activation entropy, particularly for the reaction catalyzed by the 'heavy' enzyme, because the corresponding recrossing coefficient is often further deviated from unity (i.e., $\gamma^{HE} < \gamma^{LE} < 1$). This effect can be counteracted by the second term $(RT/\gamma)\cdot(\partial\gamma/\partial T)$, which accounts for the temperature dependence of dynamic recrossing. It should be noted that the entropy of activation in eq 3 is not the total entropy of activation given in Table 2, but only the recrossing-dependent component. Here, $\Delta S_{\gamma}^{\ddagger}$ only refers to the mass-dependent contribution, whereas $\Delta S^{\ddagger}$ in Table 2 is composed of both mass-dependent factors and other contributions that are insensitive to enzyme isotope substitutions.

As illustrated in Figure 2B, the 'heavy' BsDHFR exhibits a sharper increase of $\gamma$ with respect to temperature, i.e., $(\partial\gamma^{HE}/\partial T) \gg (\partial\gamma^{LE})/(\partial T)$, and a smaller value of $\gamma$, thus rendering a larger (positive) value for the second term of eq 3, which lowers the absolute value of $\Delta S^{\ddagger}$ for hydride transfer (making it less negative). The resulting entropy−enthalpy compensation (see Table 2) means that the activation free energies for the reactions catalyzed by the 'light' and 'heavy' enzymes are very similar. As the magnitude of $\gamma$ is sensitive to changes of the protein environmental motions along the reaction coordinate,


dx.doi.org/10.1021/ja5102536 | J. Am. Chem. Soc. 2014, 136, 17317−17323

the flexibility of BsDHFR likely accounts for the changes of these activation parameters. At high temperatures, although mass-dependent vibrational frequencies are lowered by enzyme isotope substitution, electrostatic preorganization in BsDHFR remains optimal and merits minimal probability of dynamic recrossing. At low temperatures, differences due to isotope-dependent protein motions become more evident between the 'light' and 'heavy' enzymes. The motion along the reaction coordinate is reduced at low temperatures, thus the hydride transfer step experiences more detrimental effects from the protein motions that reorganize the active site. This analysis clearly demonstrates that protein motions have distinct effects at different stages of catalysis: enzyme flexibility is critical during the process of preorganization, yet too much flexibility could perturb the stability of the TS.

The current and previous studies[7,8] of DHFRs have demonstrated that a TST framework corrected for dynamic recrossing can satisfactorily reproduce both the enzyme KIEs and their temperature dependence. These results demonstrate the reliability of this approach to characterize the enzyme TS. In addition, the present work provides a plausible rationale for why dynamic coupling might differ among homologues, offering a systematic way to analyze this effect according to the terms appearing in eq 3. For EcDHFR, the slight temperature-dependent increase of the enzyme KIE[7] likely implies the dominance of $R{\cdot}\ln(\gamma)$ in eq 3, which leads to a slightly larger magnitude of $\Delta S^{\ddagger}$ for the 'heavy' enzyme (Table 2). This would be in agreement with a relatively low flexibility of the protein environment along the reaction coordinate for this enzyme. EcDHFR-N23PP/S148A is less well set up for the hydride transfer reaction and so contains additional fast protein motions in the TS.[8] These factors are reflected in a noticeable increase in the magnitude of $\Delta S^{\ddagger}$ relative to wild-type EcDHFR and a relatively high enzyme KIE (~1.35). However, $\Delta S^{\ddagger}$ is the same in 'light' and 'heavy' EcDHFR-N23PP/S148A, presumably because, despite the first term of eq 3 being more different between 'light' and 'heavy' in this enzyme[8] than in the wild-type,[7] there is a stronger temperature-dependent variation in the recrossing transmission coefficients such that changes to the two terms in eq 3 partially cancel one another. Finally, the enzyme KIE for TmDHFR was 1 at all temperatures.[9] Following the same arguments, both terms of eq 3 would be equal for the 'light' and 'heavy' enzymes, in agreement with the same value of activation entropy experimentally measured (Table 2). The structural constraints required for this enzyme to function at ~80 °C lead to a significant increase in the energy barrier for forming an ideal reactive transition-state configuration, as is evidenced by the higher value of $\Delta H^{\ddagger}$. This outweighs the effect of the protein environmental fluctuations. Together, we conclude that the strength of a dynamic effect is reflected in the differences observed in the activation parameters, which in turn rely on the nature of the active site, the fast protein dynamics that are relevant during the passage over the chemical barrier (e.g., the difference between $\gamma^{HE}$ and $\gamma^{LE}$), and the structural flexibility of the enzyme that could affect catalysis (e.g., the magnitude of $\partial\gamma/\partial T$). Nevertheless, regardless of its temperature dependence, dynamic effects in all the wild-type homologues are small at physiological temperatures. In our opinion, the current experimental/theoretical approach is a systematic method to analyze the nature of protein dynamics in enzyme catalysis. The generality of this proposal will be verified by examining other systems for which enzyme KIEs have been reported.[2−5]

## ■ ASSOCIATED CONTENT

### Supporting Information

Full experimental procedures; mass spectra of purified proteins; circular dichroism spectra, tabulated experimental data for $k_H$, $k_{cat}$, and enzyme KIEs, pH dependence of $k_H$; methodological details of QM/MM calculations, including PMFs, recrossing and tunneling coefficients, and quantum vibrational corrections. This material is available free of charge via the Internet at http://pubs.acs.org.

## ■ AUTHOR INFORMATION


### Corresponding Authors

allemannrk@cf.ac.uk
moliner@uji.es
ignacio.tunon@uv.es

### Author Contributions

[#]These authors have contributed equally.


### Notes

The authors declare no competing financial interest.

## ■ ACKNOWLEDGMENTS

The authors acknowledge computational resources from the University of Valencia (Tirant supercomputer) and from University Jaume I. This work was supported by grants BB/L020394/1 and BB/J005266/1 (RKA) from the UK Biotechnology and Biological Sciences Research Council (BBSRC) and EP/L027240/1 from the UK Engineering and Physical Sciences Research Council (EPSRC), by FEDER and Ministerio de Economía y Competitividad funds (project CTQ2012-36253-C03), Generalitat Valenciana (ACOMP/2014/277 and PrometeoII/2014/022) and by Universitat Jaume I (Project P1·1B2011−23).

## ■ REFERENCES


(1) Świderek, K.; Ruiz-Pernía, J. J.; Moliner, V.; Tuñón, I. *Curr. Opin. Chem. Biol.* **2014**, *21*, 11.
(2) Silva, R. G.; Murkin, A. S.; Schramm, V. L. *Proc. Natl. Acad. Sci. USA* **2011**, *108*, 18661.
(3) Pudney, C. R.; Guerriero, A.; Baxter, N. J.; Johannissen, L. O.; Waltho, J. P.; Hay, S.; Scrutton, N. S. *J. Am. Chem. Soc.* **2013**, *135*, 2512.
(4) Toney, M. D.; Castro, J. N.; Addington, T. A. *J. Am. Chem. Soc.* **2013**, *135*, 2509.
(5) Kipp, D. R.; Silva, R. G.; Schramm, V. L. *J. Am. Chem. Soc.* **2011**, *133*, 19358.
(6) Wang, Z.; Singh, P. N.; Czekster, C. M.; Kohen, A.; Schramm, V. L. *J. Am. Chem. Soc.* **2014**, *136*, 8333.
(7) Luk, L. Y. P.; Ruiz-Pernia, J. J.; Dawson, W. M.; Roca, M.; Loveridge, E. J.; Glowacki, D. R.; Harvey, J. N.; Mulholland, A. J.; Tuñón, I.; Moliner, V.; Allemann, R. K. *Proc. Natl. Acad. Sci. U.S.A.* **2013**, *110*, 16344.
(8) Ruiz-Pernia, J. J.; Luk, L. Y. P.; García-Meseguer, R.; Martí, S.; Loveridge, E. J.; Tuñón, I.; Moliner, V.; Allemann, R. K. *J. Am. Chem. Soc.* **2013**, *135*, 18689.
(9) Luk, L. Y. P.; Loveridge, E. J.; Allemann, R. K. *J. Am. Chem. Soc.* **2014**, *136*, 6862.
(10) Born, M.; Oppenheimer, R. *Ann. Phys. (Berlin, Ger.)* **1927**, *389*, 457.
(11) Karplus, M.; McCammon, J. A. *Annu. Rev. Biochem.* **1984**, *52*, 263.
(12) Basran, J.; Sutcliffe, M. J.; Scrutton, N. S. *Biochemistry* **1999**, *39*, 3218.
(13) Antoniou, D.; Caratzoulas, S.; Kalyanaraman, C.; Mincer, J. S.; Schwartz, S. D. *Eur. J. Biochem.* **2002**, *269*, 3103.
(14) Sutcliffe, M. J.; Scrutton, N. S. *Eur. J. Biochem.* **2002**, *269*, 3096.

(15) Knapp, M. J.; Klinman, J. P. *Eur. J. Biochem.* **2002**, *269*, 3113.
(16) Klinman, J. P. *J. Phys. Org. Chem.* **2010**, *23*, 606.
(17) Kamerlin, S. C. L.; Warshel, A. *Protein* **2010**, *78*, 1339.
(18) Adamczyk, A. J.; Cao, J.; Kamerlin, S. C. L.; Warshel, A. *Proc. Natl. Acad. Sci. U.S.A.* **2011**, *108*, 14115.
(19) Boekelheide, N.; Salomón-Ferrer, R.; Miller, T. F. *Proc. Natl. Acad. Sci. U.S.A.* **2011**, *108*, 16159.
(20) Loveridge, E. J.; Tey, L.-H.; Allemann, R. K. *J. Am. Chem. Soc.* **2010**, *132*, 1137.
(21) Loveridge, E. J.; Behiry, E. M.; Guo, J.; Allemann, R. K. *Nat. Chem.* **2012**, *4*, 292.
(22) Oyeyemi, O. A.; Sours, K. M.; Lee, T.; Kohen, A.; Resing, K. A.; Ahn, N. G.; Klinman, J. P. *Biochemistry* **2011**, *50*, 8251.
(23) Francis, K.; Stojković, V.; Kohen, A. *J. Biol. Chem.* **2013**, *288*, 35961.
(24) Singh, P.; Sen, A.; Francis, K.; Kohen, A. *J. Am. Chem. Soc.* **2014**, *136*, 2575.
(25) Pisliakov, A. V.; Cao, J.; Kamerlin, S. C. L.; Warshel, A. *Proc. Natl. Acad. Sci. U.S.A.* **2009**, *106*, 17359.
(26) Pu, J.; Ma, S.; Gao, J.; Truhlar, D. G. *J. Phys. Chem. B* **2005**, *109*, 8551.
(27) Cui, Q.; Karplus, M. *J. Phys. Chem. B* **2002**, *106*, 7927.
(28) Basran, J.; Sutcliffe, M. J.; Scrutton, N. S. *J. Biol. Chem.* **2001**, *276*, 24581.
(29) Hay, S.; Pang, J. Y.; Monaghan, P. J.; Wang, X.; Evans, R. M.; Sutcliffe, M. J.; Allemann, R. K.; Scrutton, N. S. *ChemPhysChem* **2008**, *9*, 1536.
(30) Hay, S.; Evans, R. M.; Levy, C.; Loveridge, E. J.; Wang, X.; Leys, D.; Allemann, R. K.; Scrutton, N. S. *ChemBioChem* **2009**, *10*, 2348.
(31) Henzler-Wildman, K.; Lei, M.; Thai, V.; Kerns, S. J.; Karplus, M.; Kern, D. *Nature* **2007**, *450*, 913.
(32) Boehr, D. D.; McElheny, D.; Dyson, H. J.; Wright, P. E. *Science* **2006**, *313*, 1638.
(33) Bhabha, G.; Lee, J.; Ekiert, D. C.; Gam, J.; Wilson, I. A.; Dyson, H. J.; Benkovic, S. J.; Wright, P. E. *Science* **2011**, *332*, 234.
(34) Frauenfelder, H.; Sligar, S.; Wolynes, P. *Science* **1991**, *254*, 1598.
(35) Sawaya, M. R.; Kraut, J. *Biochemistry* **1997**, *36*, 586.
(36) Dams, T.; Auerbach, G.; Bader, G.; Jacob, U.; Ploom, T.; Huber, R.; Jaenicke, R. *J. Mol. Biol.* **2000**, *297*, 659.
(37) Kim, H. S.; Damo, S. M.; Lee, S. Y.; Wemmer, D.; Klinman, J. P. *Biochemistry* **2005**, *44*, 11428.
(38) Guo, J.; Luk, L. Y. P.; Loveridge, E. J.; Allemann, R. K. *Biochemistry* **2014**.
(39) Meinhold, L.; Clement, D.; Tehei, M.; Daniel, R.; Finney, J. L.; Smith, J. C. *Biochem. J.* **2008**, *94*, 4812.
(40) Fierke, C. A.; Johnson, K. A.; Benkovic, S. J. *Biochemistry* **1987**, *26*, 4085.
(41) Glasstone, S.; Laidler, K. J.; Eyring, H. *The Theory of Rate Processes: The Kinetics of Chemical Reactions, Viscosity, Diffusion and Electrochemical Phenomena*; McGraw-Hill: New York, 1941.
(42) Keck, J. C. In *Advances in Chemical Physics*; John Wiley & Sons, Inc.: Hoboken, NJ, 2007; p 85.
(43) Truhlar, D. G.; Garrett, B. C.; Klippenstein, S. J. *J. Phys. Chem.* **1996**, *100*, 12771.
(44) Alhambra, C.; Corchado, J.; Sánchez, M. L.; Garcia-Viloca, M.; Gao, J.; Truhlar, D. G. *J. Phys. Chem. B* **2001**, *105*, 11326.